Composites Part B 122 (2017) 145–155

Contents lists available at ScienceDirect

Composites Part B

journal homepage: www.elsevier.com/locate/compositesb

Polymer composites-based thermoelectric materials and devices

Liming Wang [a], Yuchen Liu [a], Zimeng Zhang [a], Biran Wang [a], Jingjing Qiu [b], David Hui [c], Shiren Wang [a,*]

[a] Department of Industrial and Systems Engineering, Texas A&M University, College Station, TX 77843, United States
[b] Department of Mechanical Engineering, Texas Tech University, Lubbock, TX 79403, United States
[c] Department of Mechanical Engineering, University of New Orleans, LA, United States

ARTICLE INFO

Article history:
Received 23 February 2017
Accepted 26 April 2017
Available online 27 April 2017

ABSTRACT

Polymer thermoelectric materials have attracted increasing attention and exhibited great potential in green energy conversion due to their inexpensive to process, lightweight, mechanical flexibility, and intrinsic low thermal conductivity in the past decades. Integration of polymers with nanofillers has been one main approach to tailor the thermoelectric properties of polymers, which not only combines the properties of each component but also displays interesting transport phenomenon induced by the interfaces between polymers and nanofillers. In this review, we discussed the thermoelectric properties of polymer composites, especially for the conducting polymer based composites, including polymer/inorganic, polymer/carbon nanofillers, polymer/polymer hybrids. The fabrication and structure-dependent thermoelectric properties were discussed. In addition, polymer composites based thermoelectric devices were also systematically addressed, and potential issues in the devices fabrication were also analyzed. Regarding the future research opportunities, some visionary discussion was also provided.

1. Introduction

Thermoelectrics, which can realize direct conversion from waste heat to electricity through Seebeck effect or be used as solid-state cooler through Peltier effect, could play an important role in solving the increasingly serious energy crisis [1,2]. The conversion efficiency of thermoelectrics is closely related to a dimensionless figure of merit, which is defined as $ZT = S^2\sigma T/\kappa$, where S is the Seebeck coefficient, σ is the electrical conductivity, κ is the thermal conductivity and T is the absolute temperature, respectively. Conventional inorganic semiconductors such as Bi_2Te_3, PbTe, SiGe, $CoSb_3$, Cu_2Se, and SnSe have attracted the most attentions due to their excellent thermoelectric properties ($ZT > 1$). However, both the high cost and the difficulty in processing restrict the wide application of these inorganic thermoelectric materials [3–5].

Polymer materials are regarded as potential alternatives due to their inexpensive to process, light weight, mechanical flexibility, and intrinsic low thermal conductivity [6,7]. Their room-temperature thermoelectric properties have been widely studied in the past decades. The most common polymer thermoelectric materials are conjugated conducting polymers which exhibit adjustable electrical conductivity within a large range based on the doping level, such as polyacetylene (PA) [8], polypyrrole (PPy) [9], polythiophene (PTh) [10], poly(3,4-ethylenedioxythiophene) (PEDOT) [11–14], poly(3-hexylthiophene) (P3HT) [15,16], and polyaniline (PANI) [17–19] as shown in Fig. 1. But similar to conventional inorganic thermoelectric materials, the electrical conductivity, Seebeck coefficient and thermal conductivity of these polymers are strongly correlated. For example, increasing electrical conductivity of polymers by heavily doping usually lead to a very low Seebeck coefficient. It is very difficult to individually tune one parameter without affecting another, thereby resulting in weak thermoelectric properties for the vast majority of polymers.

Recently, compounding nanofillers with polymers has emerged as an effective way to decouple those thermoelectric parameters and yield factorial enhancement in power factor ($S^2\sigma$) or ZT value, owing to the combination of unique properties of each components and the fascinating electrical/thermal transport phenomenon at the interfaces [20–25]. Therefore, polymer thermoelectric composites have been the research hotspot in the field of organic thermoelectrics. Furthermore, the mechanical flexibility and solution processibility of polymer composites provide more inexpensive fabrication methods for thermoelectric devices and enable these devices possessing wider applications such as flexible wearable

* Corresponding author.
E-mail address: s.wang@tamu.edu (S. Wang).

http://dx.doi.org/10.1016/j.compositesb.2017.04.019
1359-8368/

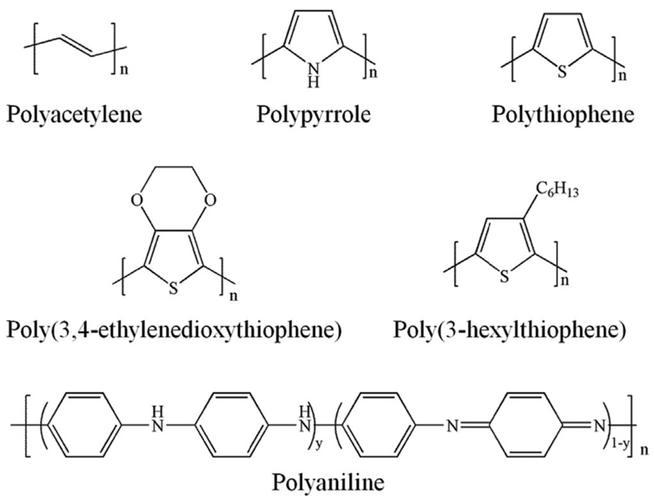

Fig. 1. Chemical structures of some common conducting polymers.

electronics, as compared to inorganic thermoelectric materials.

Herein, we focus on recent progress on polymer composites based thermoelectric materials and devices in this review. We start from the thermoelectric properties of polymer composites, highlight interesting electrical/thermal transport results in some typical polymer composites, and discuss the underlying mechanisms for those phenomena. Then, polymer composites based thermoelectric devices are summarized. Finally, brief conclusions and some outlooks for future investigation are presented.

2. Thermoelectric properties of polymer composites

To implement the fabrication of polymer thermoelectric composites, two classes of nanofillers are applied generally [5]. One class of fillers are inorganic particles including Te nanorods [23,26–28], SnSe [29,30] and Bi_2Te_3 [31–33], exhibiting high Seebeck coefficient. Another mostly used class of filling materials are carbon particles such as carbon nanotubes (CNTs) [34–37] and graphene [38–40], possessing high electrical conductivity. In this part, we mainly introduce the thermoelectric properties of polymer/inorganic particle composites and polymer/carbon particle composites and compare the features of these two types of composites. In addition, polymer/polymer composites are highlighted, which display the unique advantages as thermoelectrics. At last, some other polymer composites are also covered such as ternary polymer/carbon particle/inorganic particle composites. Table 1 lists the room-temperature thermoelectric properties and synthesis methods of some selected typical polymer composites. Through researchers' continuous efforts, a number of polymer composites with high thermoelectric power factor (>100 $\mu W\ m^{-1}\ K^{-2}$) are reported [20,26,30,33–35,37,41–48]. Most polymer thermoelectric composites are prepared based on solution process, mainly including direct solution mixing and in situ polymerization methods. Thin film samples are obtained after drop-casting or spin-coating with the solution.

2.1. Polymer/inorganic nanopartical composites

Compared with the best inorganic thermoelectric material at room temperature, Bi_2Te_3, conducting polymers can display an electrical conductivity at the same level and a much lower thermal conductivity. While the Seebeck coefficient of polymers is not facile to adjust. In order to significantly improve the Seebeck coefficient, researchers attempted to compound polymers with thermoelectrically active materials [5,26,29,30,32,33,51,52,61]. Moreover, potential carrier filtering was deemed to contribute the large Seebeck coefficient (163 $\mu V\ K^{-1}$) and power factor (70.9 $\mu W\ m^{-1}\ K^{-2}$) of poly(3,4-ethylenedioxythiophene):poly(styrenesulfonate) (PEDOT:PSS)/Te nanorods hybrids with numerous nanoscale interfaces [23]. Then, He et al. made use of the energy filtering effect to improve the Seebeck efficient and power factor of P3HT/Bi_2Te_3 nanocomposites by rationally engineering the polymer/inorganic interfaces [32]. Different energy barrier at the interfaces could be created by changing the doping level of P3HT. As shown in Fig. 2a, the interfacial energy barrier at the heavily doped P3HT/Bi_2Te_3 nanowire interface was below 0.1 eV, which selectively scattered carriers with low energy, thereby sharpening the effective density of states of the composites and enhancing the Seebeck coefficient. For the lightly doped P3HT/Bi_2Te_3 nanocomposites, the interfacial energy barrier greatly increased because of the much larger band gap (E_g) of lightly doped P3HT (Fig. 2b). At this situation, most carriers would be scattered resulting in dramatically reduced carrier transfer and electrical conductivity. Thus, reduced Seebeck coefficient and power factor were observed in nanocomposites with lightly doped P3HT matrix. Afterwards, capitalizing on the benefits of energy filtering effect was also accomplished in other polymer/inorganic particle systems, such as PEDOT:PSS/SnSe composites [30] and PEDOT:PSS/Te-$Cu_{1.75}$Te composites [52]. The upper limit value and lower limit value for the Seebeck coefficient of PEDOT:PSS/SnSe composites were calculated according to series-connected model and parallel-connected model without considering the interfaces. Interestingly, the experimental Seebeck coefficient values of PEDOT:PSS/SnSe composites were much larger than the calculated values based on both models. The enhancement in Seebeck coefficient was ascribed to the energetic mismatches at the interfaces between polymer and inorganic particles. Finally, the PEDOT:PSS/SnSe composites with 20 wt% SnSe exhibited a maximum ZT value of 0.32 at room temperature.

Apart from commonly used energy filtering effect, Lee et al. applied modulation doping strategy to improve the thermoelectric properties of PEDOT:PSS/undoped Si (001) nanoscale heterostructures not long ago [53]. Fig. 3 gives schematic comparison of the energy filtering mechanism and the modulation doping mechanism. Unlike the former one, modulation doping can be a principle of work in the planar transport direction, as shown in Fig. 3c. The charge carriers can transfer from a more doped material to adjacent less doped material with high mobility [62,63], without decreasing the Seebeck coefficient. As a result, a larger Seebeck coefficient up to 7.3 fold and a larger power factor up to 17.5 fold in comparison to PEDOT:PSS were received in PEDOT:PSS/undoped Si (001) nanocomposites.

Although quite a lot of polymer/inorganic composites have presented much high Seebeck coefficient, their electrical conductivity values cannot meet the demands. The main challenge is the difficulty to form a intimate interfacial connection between polymers and inorganic particles due to the lack of effective interactions [64]. This greatly restricts the carrier transport in polymer/inorganic composites. For example, the composites of PEDOT:PSS mixed with p-type Bi_2Te_3 powders showed an electrical conductivity around 100 S cm^{-1}, which was one order of magnitude lower than both PEDOT:PSS and Bi_2Te_3 [33]. Moreover, the value was also much lower than the lower limit value estimated by the series connect model. This low electrical conductivity was thought to arise from the large interfacial resistance between PEDOT:PSS and Bi_2Te_3 powders.

On the other hand, relatively low thermal conductivity values are supposed due to the low electrical conductivity and weak interactions between polymers and inorganic particles. The in-plane

Table 1
A summary of room-temperature thermoelectric properties for selected typical polymer composites.

Materials	σ (S cm-1)	S (μV K^{-1})	PF (μW m^{-1} K^{-2})	κ (W m^{-1} K^{-1})	ZT	Synthesis method	Ref.
Part I: Polymer/inorganic particle composites							
PEDOT/Te	19.3	163	70.9	0.22–0.3 ⊥		In situ synthesis	[23]
PEDOT/Te	11	180	35	0.16 ⊥		In situ synthesis	[49]
PEDOT/Te	2	150	4.5			In situ synthesis	[50]
PEDOT/Te	115	215	284			In situ synthesis	[45]
PANI/Te	102	102	105	0.21 ⊥		Solution mixing	[26]
PEDOT/Bi_2Te_3	~62	~145	131			Solution mixing	[33]
PANI/Bi_2Te_3	11.6	~36	~1.5	0.1 ⊥		In situ polymerization	[31]
P3HT/Bi_2Te_3	~10	~117	13.6	0.54–0.86		Solution mixing	[32]
PEDOT/MoS_2	1250	19.5	45.6	0.27 ⊥		Solution mixing	[51]
PEDOT/Te-$Cu_{1.75}$Te	~17.4	~220	84			In situ synthesis	[52]
PEDOT/SnSe	~320	~110	~380	~0.36	0.32	Solution mixing	[30]
PEDOT/Si	49	73	26.2			Spin-coating	[53]
Part II: Polymer/carbon particle composites							
PANI/MWNTs	61.47	28.6	5.04	0.5	0.003	In situ polymerization	[22]
PANI/SWNTs	125	40	20	1.5	0.004	In situ polymerization	[21]
PANI/SWNTs	769	65	176	0.43 ⊥		Solution mixing	[20]
PANI/DWNTs	610	61	220			Solution mixing	[35]
PANI/SWNTs	1440	38.9	217	0.44 ⊥		In situ polymerization	[34]
PANI/graphene	856	15	19			Solution mixing	[54]
PANI/graphene	814	26	55			In situ polymerization	[39]
PEDOT/SWNTs	1000	18–34	160			Solution mixing	[37]
PEDOT/DWNTs	780	43.7	151			Solution mixing	[55]
PEDOT/graphene	~1160	~17	32.6			Solution mixing	[56]
PEDOT/graphene	637	26.8	45.7			In situ polymerization	[40]
P3HT/SWNTs	~1100	~29	95			Solution mixing	[36]
P3HT/SWNTs	2760	31.1	267			Solution mixing bar-coating	[47]
PS/SWNTs	1250	58	413	0.3 ⊥		Solution mixing	[46]
PEDOT/graphene /C_{60}	~720	~34	83.2	0.25 ⊥		Solution mixing	[57]
PANI/graphene /PANI/DWNTs	1080	130	1825			Layer by Layer assembly	[48]
PANI/graphene /PANI/DWNTs	1900	120	2710			Layer by Layer assembly	[44]
Part III: Polymer/polymer composites							
P3BT/PS	0.002	600	0.07	0.25	0.00008	Solution mixing	[58]
PEDOT/P3HT	200.5	17	5.8			Electrochemical polymerization	[59]
PEDOT/PANI	1585	17.5	49			Layer by Layer deposition	[60]
PEDOT/PEDOT	1270	59.3	446.6	0.26 ⊥		Vapor phase polymerization	[42]
Part IV: Other polymer composites							
PEDOT/graphene/Te	35	202	143	0.21 ⊥		Solution mixing	[43]
PANI/SWNTs/Te	345	54	101	0.3 ⊥		In situ polymerization	[41]

Abbreviation⊥ represents that the thermal conductivity is measured in the out-of-plane direction which is perpendicular to the measurement direction of the electrical conductivity and Seebeck coefficient; SWNTs = single-walled carbon nanotubes; DWNTs = double-walled carbon nanotubes; MWNTs = multi-walled carbon nanotubes; P3BT = poly(3-butylthiophene); PS = polystylene.

thermal conductivity of P3HT/Bi_2Te_3 nanocomposite films were measured by the transient electrothermal technique [32]. The values kept at a low level even for the composite film with 20 wt% Bi_2Te_3 nanowires (κ = 0.86 W m^{-1} K^{-1}), just slightly higher than the thermal conductivity of polymer matrix (κ = 0.54 W m^{-1} K^{-1}). The in-plane thermal conductivity of PEDOT:PSS/SnSe nanosheets

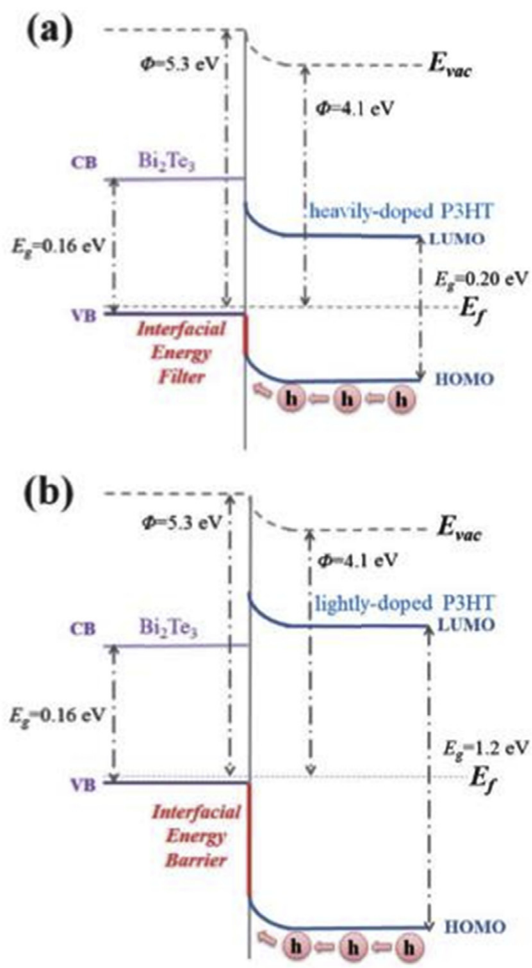

Fig. 2. The band diagram of (a) heavily doped P3HT/Bi_2Te_3 interface and (b) lightly doped P3HT/Bi_2Te_3 interface [32].

composite films were also investigated using a LFA 447 Nanoflash equipment [30]. The thermal conductivity values were only increased from 0.25 W m^{-1} K^{-1} to 0.45 W m^{-1} K^{-1} when the loading of SnSe nanosheets ranged from 0 wt% to 50 wt%, which was much insensitive to the SnSe content compared with the electrical conductivity and Seebeck coefficient. These low thermal conductivity values were ascribed to the strong phonon scattering at the interfaces in polymer/inorganic particle composites, thereby promoting the achievement of excellent thermoelectric performance.

2.2. Polymer/carbon particle composites

In 2010, Yao et al. and Meng et al. respectively reported the thermoelectric properties of PANI/SWNTs and PANI/MWNTs composites for the first time [21,22]. The electrical conductivity and Seebeck coefficient of the composites simultaneously increased with the increase of CNTs. These results supply new opportunities to synergistically tune thermoelectric parameters for better properties, which is very difficult for conventional inorganic bulks. Therefore, carbon particles, especially SWNTs, DWNTs and graphene, have emerged as the leading additives for improving the thermoelectric properties of polymers in recent years.

Generally, high electrical conductivity can be obtained in polymer/carbon particle composites when the content of carbon particles exceeds the percolation threshold to form conductive networks [36,37,56,65,66]. Another distinguishing feature in polymer/carbon particle composites is the strong π-π interactions between polymers and carbon particles, which are found to have great influence on the electrical transport properties of the composites [20,21,34,39,67–71]. For instance, PANI/SWNTs composite films with high thermoelectric properties were prepared with CSA doped PANI, SWNTs powders and m-cresol solvent by the directly solvent mixing [20]. It was found that highly ordered PANI interface layers formed on the SWNT surfaces, which were induced by the synergetic effect of chain expansion by the chemical interactions between PANI and the solvent and the π–π conjugation between PANI and SWNTs. Thus, the carrier mobility as well as electrical conductivity of the composite film were greatly enhanced. The electrical conductivity of PANI/SWNTs composite film reached 769 S cm^{-1}, which was much higher than the value calculated based on the series-connected two-component mixture model. Similar results were also reported in other polymer/carbon particle composites [34,69]. In consequence, polymer/carbon particle composites commonly exhibit very high electrical conductivity, not only result from the contribution of the highly conductive carbon particles, but also due to the enhanced ordered degree of polymers.

Besides, these carbon based nanofillers have unique morphology, quasi-one-dimensional nanostructure for CNTs and two-dimensional planar nanostructure for graphene. Similar to polymer/inorganic particle composites, energy filtering effect would arise when carriers cross the interfaces between polymers and carbon particles. Meng et al. prepared PANI/CNTs composites

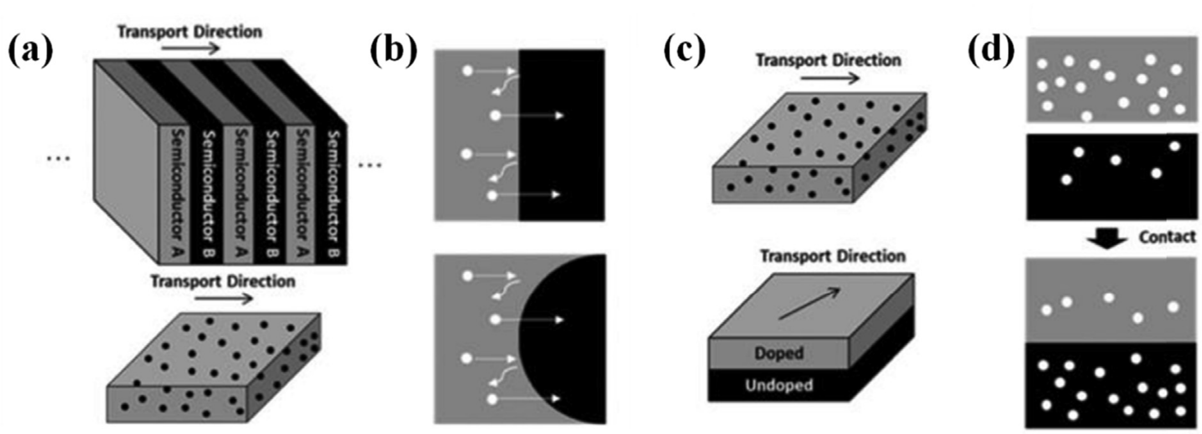

Fig. 3. Schematic comparison of (a, b) the energy filtering mechanism and (c, d) the modulation doping mechanism [53].

by in situ polymerization method with different forms of CNTs (CNT sheet, CNT pellet and CNT array), all of which displayed much enhanced Seebeck coefficient as compared to the pristine CNT arrays or pure PANI [22]. This unconventional improvement in Seebeck coefficient was considered to be caused by a size-dependent energy filtering effect since the CNTs were enwrapped by the uniform PANI layer at the nanoscale. Later, our group developed a novel method to modulate the energy barrier between polymer matrix and carbon fillers and achieved high thermoelectric performance in PEDOT:PSS/carbon particle composites [57]. Firstly, fluorinated C_{60} (F-C_{60}) with a deep highest occupied molecular orbital (HOMO) level was used to decorate reduced graphene oxide (rGO), as presented in Fig. 4a. Modulated HOMO level of rGO/F-C_{60} hybrids was expected by tailoring the F-C_{60} content on rGO (Fig. 4b). Thus, different energy barrier would be constructed at the interface between PEDOT:PSS and rGO/F-C_{60}. Fig. 4c and d plotted the Seebeck coefficient and electrical conductivity of PEDOT:PSS/rGO/F-C_{60} composites as a function of interfacial energy barrier. The electrical conductivity of composites decreased as the barrier height, because more low-energy carriers were scattered at the interfaces. On the contrary, most Seebeck coefficient values increased with the increase of barrier height. As a result, the optimal power factor was up to 83.2 μW m^{-1} K^{-2} for PEDOT:PSS/rGO/F-C_{60} composites.

New fabrication method has also been adopted to prepare polymer/carbon particle composites with special structure in order to optimize their thermoelectric properties most recently. Grunlan et al. prepared PANI/graphene/PANI/DWNTs nanocomposites with ordered molecular structure using layer by layer deposition method [48]. The electrical conductivity and Seebeck coefficient simultaneously increased with the increase of layers. Finally, the maximum electrical conductivity, Seebeck coefficient and power factor reached 1080 S cm^{-1}, 130 μV K^{-1} and 1825 μW m^{-1} K^{-2}, respectively. When using conductive PEDOT:PSS to stabilize graphene and DWNTs and preparing PANI/graphene-PEDOT:PSS/PANI/DWNTs-PEDOT:PSS composite thin films by layer by layer assembly technique, the electrical conductivity and power factor further increased to 1900 S cm^{-1} and 2710 μW m^{-1} K^{-2}, respectively [44]. This is the largest power factor for oganic thermoelectrics so far.

Nonetheless, an issue can not be dodged is the unknown in-plane thermal conductivity for those polymer/carbon particle composite films with high thermoelectric power factor. Most literature about polymer/carbon particle composites do not show the thermal conductivity or estimated ZT value with the out-of-plane thermal conductivity as shown in Table 1, since it is still challenging to accurately obtain the in-plane thermal conductivity of these thin films [72]. Considering their large aspect ratios, CNTs and graphene are likely to align along the in-plane direction during preparation process. Thus, obvious anisotropic thermal conductivity should exist in polymer/carbon particle composites. Mai and coworkers fabricated conjugated polyelectrolytes/SWNTs composite films and specially investigated their thermal conductivity in both in-plane and out-of-plane direction [73]. It was found the in-plane thermal conductivity of these composites was approximately an order of magnitude larger than that value in out-of-plane direction. Chen et al. also reported strong anisotropic electrical and thermal transport properties in PANI/CNTs composites very recently [74]. These results prompt to consider the influence of anisotropy when studying the thermoelectric properties of polymer/carbon particle composites in the future.

2.3. Comparison between polymer/inorganic particle composites and polymer/carbon particle composites

The properties of polymer composites depend on the properties of each components as well as the interfacial transport properties. Here we make a brief comparison between the current two major types of polymer composites with high thermoelectric power factor in Table 2. Also, their room-temperature Seebeck coefficient as function of electrical conductivity are plotted in Fig. 5. For the

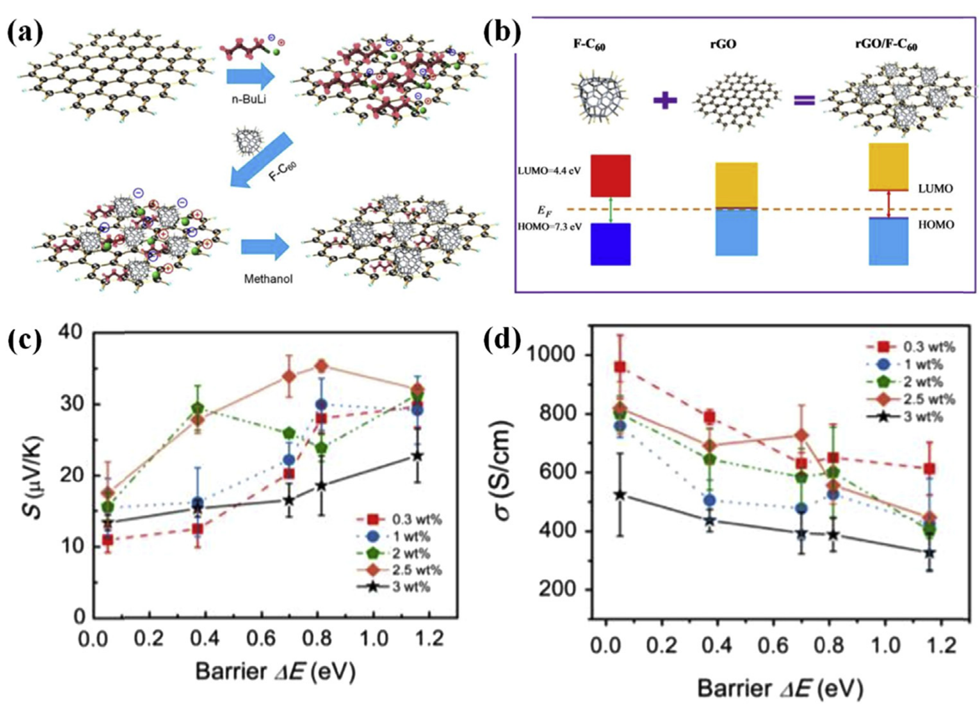

Fig. 4. (a) Illustration of preparation procedure for rGO/F-C_{60} nanohybrids through lithiation reaction. (b) Illustration of F-C_{60} modulating the band structure of rGO. (c) The Seebeck coefficient and (d) electrical conductivity of PEDOT:PSS/rGO/F-C_{60} composites as a function of barrier height [57].

Table 2
A summary of the features for polymer/inorganic particle thermoelectric composites and polymer/carbon particle thermoelectric composites with high thermoelectric power factor at room temperature.

Sample	Advantages	Disadvantages
Polymer/inorgaic particle composites	Very high S; Relatively low κ	Weak interaction at the interfaces; Low σ; High weight; Brittle
Polymer/carbon particle composites	Strong interaction at the interfaces; Very high σ; Light weight	Low S; Possible much high κ

polymer/inorganic particle composites, most of the Seebeck coefficient values are very high (>100 μV K^{-1}), while the electrical conductivity are very low (<100 S cm^{-1}) due to the weak interaction at the interfaces between polymers and inorganic particles. In turn, the low conductivity and interfacial mismatch contribute to relatively low thermal conductivity of polymer/inorganic particle composites. In order to achieve high thermoelectric properties, large loading of fillers tends to be needed in polymer/inorganic composites. This leads to the high weight of the composites, sacrifices the mechanical flexibility, and makes them brittle. As to the polymer/carbon particle composites, SWNTs, DWNTs and graphene are the leading additives for improving the thermoelectric properties. Their light weight, excellent mechanical properties and electronic transport properties generally result in flexible composites with very high electrical conductivity (>100 S cm^{-1}). Furthermore, strong π-π interactions between polymers and those carbon materials with sp2 hybridized carbon atoms can increase the electrical conductivity by providing conductive path at the interfaces and inducing more extended polymer molecular chains. However, most of the Seebeck coefficient values polymer/carbon particle composites are relatively low (<50 μV K^{-1}). Meanwhile, the high thermal conductivity of carbon particles and their orientation arrangement along the in-plane direction may cause much high in-plane thermal conductivity of polymer/carbon particle composites. Both of them go against excellent thermoelectric properties in polymer/carbon particle composites.

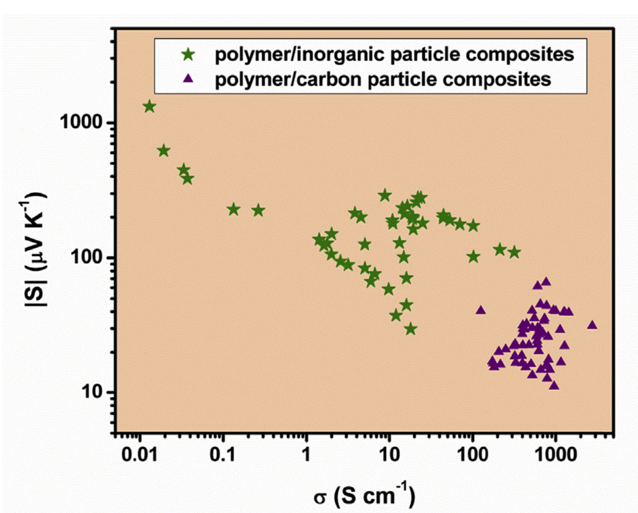

Fig. 5. Seebeck coefficient as function of electrical conductivity for a rang of selected polymer/inorganic particle composites and polymer/carbon particle composites with high thermoelectric power factor at room temperature. The plots include polymer/Te composites [23,26,45,49,50], polymer/Bi_2Te_3 composites [31–33,75], polymer/SnSe composites [29,30], polymer/Te-$Cu_{1.75}$Te composites [52], polymer/Si composites [53], polymer/$Bi_{0.5}Sb_{1.5}Te_3$ composites [76,77], polymer/Bi_2S_3 composites [78], polymer/PbTe composites [79], polymer/SWNTs composites [20,21,34,36,37,46,47], polymer/DWNTs composites [35,55], polymer/graphene composites [38–40,54,56], and polymer/C_{60}/graphene composites [57].

2.4. Polymer/polymer composites

Recently, preparation of polymer/polymer composites provided new chance to improve the thermoelectric properties [58–60,80]. This type of composites has its unique features as thermoelectrics, as compared to polymer/inorganic particle composites and polymer/carbon particle composites mentioned above. Polymer/polymer thermoelectric composites not only keep good mechanical flexibility and light weight, but also show further decreased thermal conductivity due to the introduction of interfaces and the relatively low thermal conductivity of polymer fillers. These features allow researchers to only focus most of energy on the electrical conductivity and Seebeck coefficient of polymer/polymer composites.

For example, Lu et al. prepared several insulating polymer/conjugated polymer composites and studied their thermoelectric properties [58]. They took P3BT/PS composites as an example and found that interpenetrating network of conjugated polymer formed in the insulating matrix, which made the composites show higher electrical conductivity and lower thermal conductivity without sacrificing Seebeck coefficient. The enhanced electrical conductivity of the composites was attributed to full crystallization of P3BT into nanowires, which provided conductive pathways for carriers. Besides, the authors reported that the 1D charge transport maximally kept the local thermal potential in P3BT/PS composites with interpenetrating network, resulting in a similar Seebeck coefficient with neat P3BT.

However, the interfacial energy filtering effect did not seem to work in greatly enhancing the Seebeck coefficient and power factor of these polymer/polymer composites. In order to unravel the underlying mechanism, our group studied the thermoelectric properties of PEDOT/PEDOT nanowire composites by a synergistic of computational and experimental investigation [81]. The results were shown in Fig. 6. It was demonstrated that the energy filtering effect in polymer/polymer composites was strongly dependent on the host mobility besides the interfacial energy barrier. The interfacial carrier scattering would play a part in a significant enhancement of the Seebeck coefficient and power factor only when the host mobility was above a critical value (~1 cm^2 V^{-1} s^{-1} for PEDOT based polymers). After further optimizing the infacial energy barrier and filler content, a maximum power factor as high as 446.6 μW m^{-1} K^{-2} was obtained for PEDOT:Tos/PEDOT nanowire composites [42].

2.5. Other polymer composites

In addition, ternary polymer/carbon particle/inorganic particle composites have been rationally designed most recently for the purpose of simultaneously obtaining high electrical conductivity, high Seebeck coefficient and low thermal conductivity in polymer composites [41,43]. A free-standing paper of PEDOT:PSS/rGO/Te composites with high thermoelectric properties and superior mechanical flexibility was fabricated through vacuum filtration of

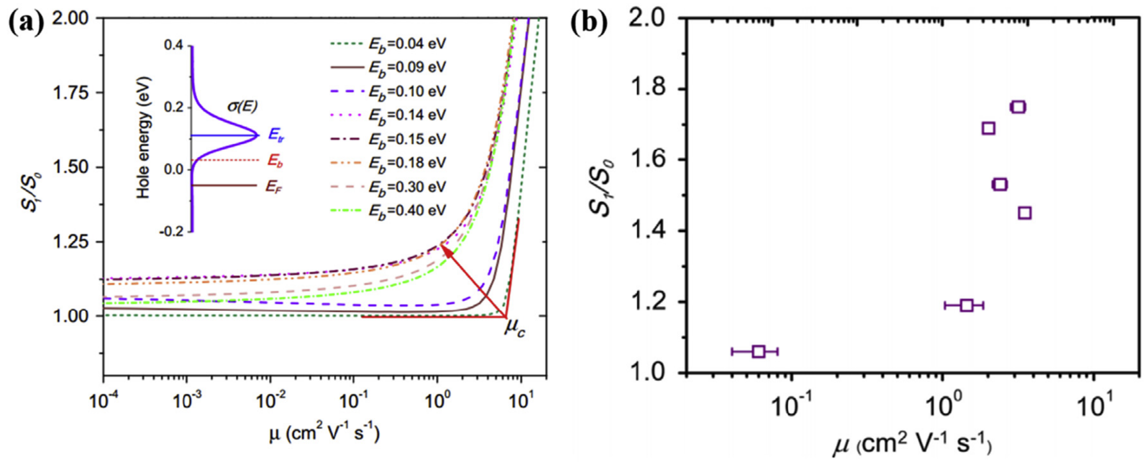

Fig. 6. (a) Computational results and (b) experimental results of the enhancement of Seebeck coefficient (S_1/S_0) as a function of carrier mobility (μ) for PEDOT based host polymers compositing with 0.2 wt% PEDOT nanowires. S_1 is the Seebeck coefficient of the host polymer with 0.2 wt% PEDOT nanowires, S_0 is the Seebeck coefficient of the host polymer without fillers [81].

suspensions [43]. The electrical conductivity drastically increased after HI treatment while the Seebeck coefficient kept at high values, because of the double carrier-filtering at two heterojunctions in the ternary hybrids. The power factor of PEDOT:PSS/rGO/Te composites reached 143 μW m^{-1} K^{-2} at 300 K, which was one to two orders of magnitude higher than those of single components or binary composites. Similar phenomena were also found in the ternary PANI/SWNTs/Te composites. The ternary composites displayed a significantly enhanced Seebeck coefficient (54 μV K^{-1}) without a large loss of electrical conductivity (345 S cm^{-1}), thereby leading to a high thermoelectric power factor of 101 μW m^{-1} K^{-2} [41].

3. Polymer composites based thermoelectric devices

3.1. Structures

Great progress has also been made on polymer composites based thermoelectric devices. One of the main advantages for organic thermoelectric materials is the easy processibility into various shapes. Consequently, polymer composites based thermoelectric devices with different structures are developed, as summarized in Fig. 7. Present reported polymer composites based thermoelectric devices were mainly designed with planar structure (Fig. 7a and b), acting as a demonstration role [34,41,42,44,45,75,77,83–88]. And, most of the devices were made up of only p type polymer composites connected in series because of lacking stable n type thermoelectric film with comparative properties [34,41,44,45,75,77,85–88]. Suemori et al. designed a thermoelectric generator with verticle structure in order to take advantage of temperature difference in the out-of-plane direction (Fig. 7c) [89]. Besides, thermoelectric devices with multilayer structure were developed, in which p type and n type films were seperated by insulating layer (Fig. 7d) [43,90,91]. This structure could make full use of space, and lead to a large output power. Not long ago, Menon et al. constructed a radial thermoelectric generator with the optimized geometry conditions, as presented in Fig. 7e [82]. PEDOT:PSS/Te nanowire composites and poly(nickel-1,1,2,2-ethenetetrathiolate) blended with poly(vinylidene fluoride) were respectively used as p type and n type films. This structure allowed to use a hot pipe as the heat source and did not need active cooling at the other side, exhibiting great application potential.

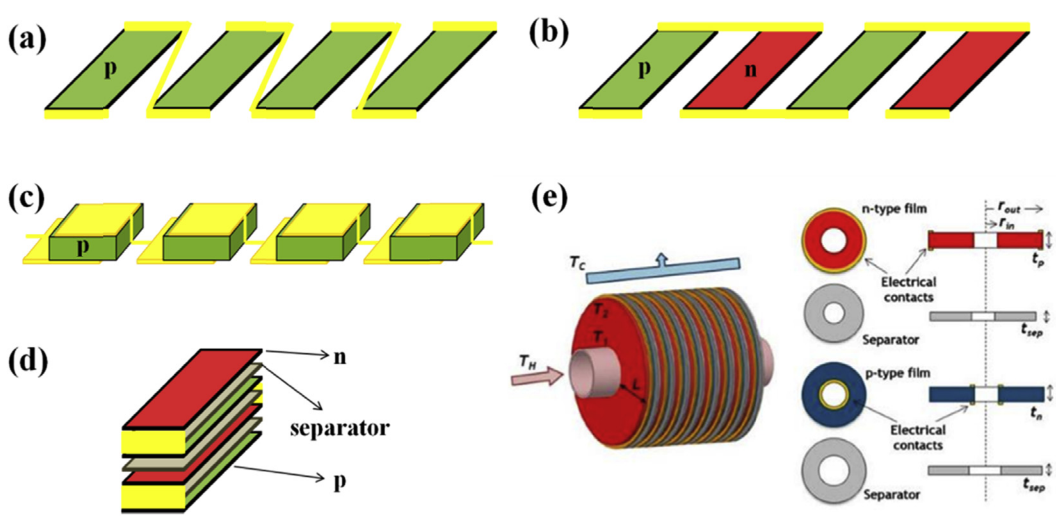

Fig. 7. Schematic illustrations of the structures for polymer composites based thermoelectric devices: (a) planar structure with p type films; (b) planar structure with both p type and n type films; (c) vertical structure with p type films; (d) multilayer structure with both p type and n type films; (e) radial structure with both p type and n type films [82]. Films are generally connected by conductive metal.

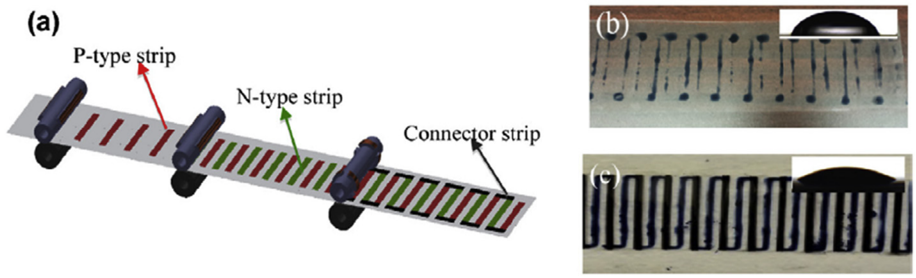

Fig. 8. (a) Illustration of roll-to-roll printing of organic thermoelectric devices; (b) UV-treated plastic substrate; and (c) plasma-treated plastic substrate [84].

3.2. Fabrication methods

Another main advantages of organic thermoelectric materials is the solution processibility. This feature makes it possible to use a lot kinds of low-cost and large-scale fabrication methods for polymer composites based thermoelectric devices. The commonly used fabrication methods for thermoelectric devices were the drop-casting and spin-coating, the same as preparation methods of materials [34,41–44,89–91]. However, these methods were not suitable for high-speed and continuous process. For this end, some printing methods were developed to produce polymer composites based thermoelectric devices. For instance, Cho's group successfully employed spray-printing method to fabricate thermoelectric devices with polymer composites, such as P3HT/CNT composites, PEDOT:PSS/Te-Bi_2Te_3 composites, and PEDOT:PSS/Te composites [45,86,87]. A mask was required in this method in order to get patterned thermoelectric materials on the substrate. Inkjet-printing method was also adopted to prepare polymer composite thermoelectric devices, which showed the advantages of without wastage of materials and masks [84,92,93]. But the problems of ink bleeding and liquid blurring should be handled by long-time post treatments.

Beyond those methods, some other methods for large-scale fabrication are also developed to print inorganic or organic thermoelectric devices such as screen printing, dispenser printing, and stereolithography [92]. Recently, our group built a roll-to-roll system for printing flexible organic thermoelectric devices [84]. As shown in Fig. 8a, three print cylinders were used to print the p type legs (PEDOT:PSS aqueous solution), n type legs (nitrogen doped graphene aqueous solution) and connector strips (PEDOT:PSS aqueous solution) in sequence. It was found that thermoelectric devices were successfully printed on the plasma-treated plastic substrate (Fig. 8c), while failed to print on the UV-treated plastic substrate due to the poor hydrophily (Fig. 8b). These low-cost, large-scale, high-speed and continuous fabrication process is of course available to manufacture polymer composites based thermoelectric devices by selecting proper inks.

3.3. Device properties

Current organic thermoelectric devices are used as generators through converting temperature difference into electricity. Here we take the device properties of the generator fabricated by 4 p type PANI/SWNTs/Te composite films as an example to show the typical

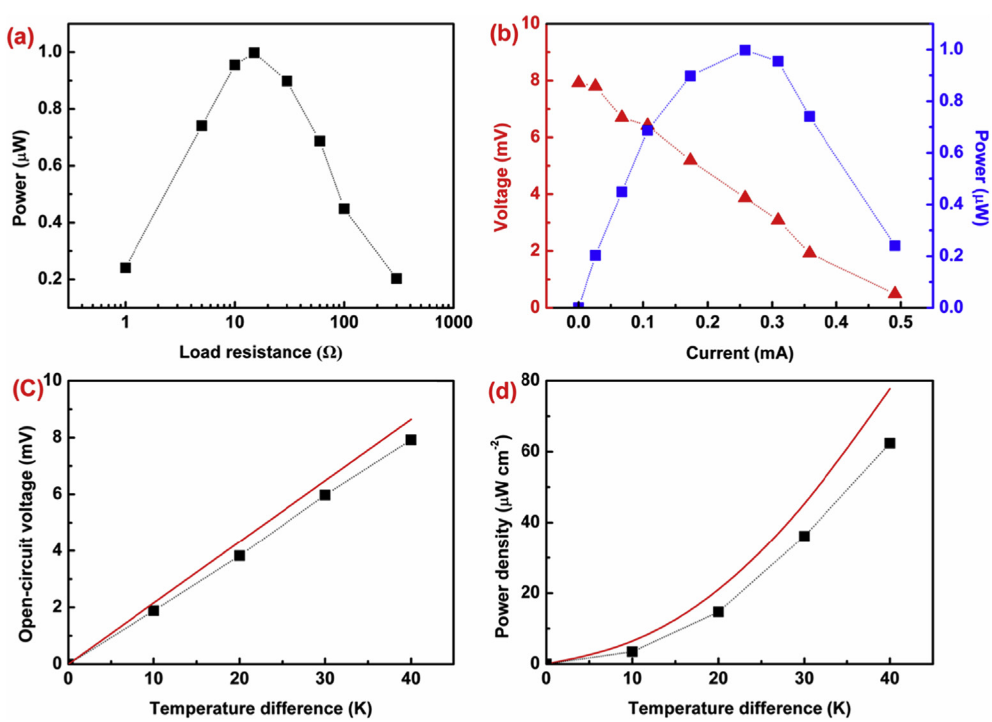

Fig. 9. Device properties of the generator fabricated by 4 p type PANI/SWNTs/Te composite films. (a) Output power of the generator as a function of load resistance at ΔT = 40 K. (b) Output voltage and power of the generator as a function of current at ΔT = 40 K. (c) Open-circuit voltage of the generator as a function of temperature difference for measured results (black solid square) and ideal model (red solid line). (d) Power density of the generator as a function of temperature difference for measured results (black solid square) and ideal model (red solid curve) [41]. (For interpretation of the references to colour in this figure legend, the reader is referred to the web version of this article.)

relationships between those parameters (Fig. 9) [41]. The output voltage can be expressed by, $U = E - IR_{in}$, where E is the open-circuit voltage of the device, R_{in} is the internal resistance of the device, and I is the output current. Then, the output power, $P = EI - I^2R_{in} = E^2R/(R + R_{in})^2$, where R is the load resistance. Therefore, the maximum output power occurs when the load resistance matches the resistance of the generator (Fig. 9a). The output voltage is inversely proportional to the output current while the output power is in parabolic curve relationship with the output current (Fig. 9b). The open-circuit voltage of the generator can be estimated by, $E = nS\Delta T$, where n is the number of the leg, S is the Seebeck coefficient of the film, and ΔT is the temperature difference. So the open-circuit voltage is proportional to ΔT, the maximum output power is proportional to ΔT^2 (Fig. 9c and d). Generally, the measured values are lower than the estimated values due to inevitable contact resistance [26,41,82,83].

In the past years, polymer composites based thermoelectric devices have shown promise in a number of applications such as self-powered wearable electronics with the improvement of device properties. A radial thermoelectric generator consisting of 15 p-n couples produced an open-circuit voltage of 85 mV and a power density of 15 nW cm^{-2} under a ΔT of 45 K [82]. Cho's group printed a thermoelectric generator containing 32 PEDOT:PSS/Te legs arranged in two rows, which produced a stable output voltage of over 2 mV using human body heat [45]. Madan et al. respectively printed epoxy/$Bi_{0.5}Sb_{1.5}Te_3$ composite thermoelectric generator and epoxy/Bi_2Te_3 composite thermoelectric generator, which displayed high power density up to 152 μW cm^{-2} and 130 μW cm^{-2} at ΔT of 20 K [75,77]. However, it should be noted that the research works about polymer composites based thermoelectric devices are still in the initial stage. The device performance is affected by a lot of factors such as the connection resistance, the geometrical shapes and sizes. It may be difficult to evaluate the present reported device properties at the same level.

4. Summary and outlook

Significant progress on polymer composites based thermoelectric materials and devices has been achieved in the past decades. Factorial enhancements in thermoelectric properties can be obtained in polymer composites as compared to the polymer matrix. Furthermore, polymer composites based thermoelectric devices have been produced by a series of solution based printing methods. These methods show obvious advantages in low-cost, large-area and high-speed fabrication.

However, there are still lots of problems to be solved in the near future. Firstly, most ZT values of polymer composite films are estimated by the out-of-plane thermal conductivity without considering the possible anistropy. It is urgent to develop some methods and techniques to accurately measure the in-plane thermal conductivity of polymer composite films. Secondly, predictive models for both electrons and phonons transport in polymer composites should be developed. Although it is difficult to find a transport model to rule polymer composites all, theoretical models built for some typical polymer composites are feasible. It will help researchers to clearly understand the underlying mechanisms of fascinating thermoelectric properties in polymer composites. Besides, new methods to design polymer composites with special and controlled nanostructures are necessary, in order to further optimize their thermoelectric properties. Finally, hybrid generators combining thermoelectric effect with other energy conversion effects based on polymer composites are greatly anticipated, which will enlarge the application of polymer thermoelectric composites in the areas of energy harvesters and energy storage devices for self-powered electronics.

Acknowledgements

Authors appreciate the support from startup funds of Texas A&M University and TEES, as well as the National Science Foundation grant (CMMI 1634858)

References

[1] Snyder GJ, Toberer ES. Complex thermoelectric materials. Nat Mater 2008;7:105–14.
[2] Zhang Q, Sun Y, Xu W, Zhu D. Organic thermoelectric materials: emerging green energy materials converting heat to electricity directly and efficiently. Adv Mater 2014;26:6829–51.
[3] Kroon R, Mengistie DA, Kiefer D, Hynynen J, Ryan JD, Yu L, et al. Thermoelectric plastics: from design to synthesis, processing and structure-property relationships. Chem Soc Rev 2016;45:6147–64.
[4] Chen Y, Zhao Y, Liang Z. Solution processed organic thermoelectrics: towards flexible thermoelectric modules. Energy & Environ Sci 2015;8:401–22.
[5] Du Y, Shen SZ, Cai K, Casey PS. Research progress on polymer-inorganic thermoelectric nanocomposite materials. Prog Polym Sci 2012;37:820–41.
[6] Russ B, Glaudell A, Urban JJ, Chabinyc ML, Segalman RA. Organic thermoelectric materials for energy harvesting and temperature control. Nat Rev Mater 2016;1:16050.
[7] He M, Qiu F, Lin Z. Towards high-performance polymer-based thermoelectric materials. Energy & Environ Sci 2013;6:1352–61.
[8] Kaneko H, Ishiguro T, Takahashi A, Tsukamoto J. Magnetoresistance and thermoelectric-power studies of metal-nonmetal transition in iodine-doped polyacetylene. Synth Met 1993;57:4900–5.
[9] Kemp NT, Kaiser AB, Liu CJ, Chapman B, Mercier O, Carr AM, et al. Thermoelectric power and conductivity of different types of polypyrrole. J Polym Sci Part B-Polymer Phys 1999;37:953–60.
[10] Lu BY, Liu CC, Lu S, Xu JK, Jiang FX, Li YZ, et al. Thermoelectric performances of free-standing polythiophene and poly(3-methylthiophene) nanofilms. Chin Phys Lett 2010;27. 057201.
[11] Bubnova O, Khan ZU, Wang H, Braun S, Evans DR, Fabretto M, et al. Semi-metallic polymers. Nat Mater 2014;13:190–4.
[12] Kim GH, Shao L, Zhang K, Pipe KP. Engineered doping of organic semiconductors for enhanced thermoelectric efficiency. Nat Mater 2013;12:719–23.
[13] Bubnova O, Berggren M, Crispin X. Tuning the thermoelectric properties of conducting polymers in an electrochemical transistor. J Am Chem Soc 2012;134:16456–9.
[14] Bubnova O, Khan ZU, Malti A, Braun S, Fahlman M, Berggren M, et al. Optimization of the thermoelectric figure of merit in the conducting polymer poly(3,4-ethylenedioxythiophene). Nat Mater 2011;10:429–33.
[15] Qu SY, Yao Q, Wang LM, Chen ZH, Xu KQ, Zeng HR, et al. Highly anisotropic P3HT films with enhanced thermoelectric performance via organic small molecule epitaxy. NPG Asia Mater 2016;8. e292.
[16] Zhang Q, Sun YM, Xu W, Zhu DB. Thermoelectric energy from flexible P3HT films doped with a ferric salt of triflimide anions. Energy & Environ Sci 2012;5:9639–44.
[17] Wang LM, Yao Q, Xiao JX, Zeng KY, Shi W, Qu SY, et al. Enhanced thermoelectric properties of polyaniline nanofilms induced by self-assembled supramolecules. Chemistry-An Asian J 2016;11:1955–62.
[18] Yao Q, Wang Q, Wang L, Wang Y, Sun J, Zeng H, et al. The synergic regulation of conductivity and Seebeck coefficient in pure polyaniline by chemically changing the ordered degree of molecular chains. J Mater Chem 2014;A 2:2634.
[19] Wang H, Yin L, Pu X, Yu C. Facile charge carrier adjustment for improving thermopower of doped polyaniline. Polymer 2013;54:1136–40.
[20] Yao Q, Wang Q, Wang L, Chen L. Abnormally enhanced thermoelectric transport properties of SWNT/PANI hybrid films by the strengthened PANI molecular ordering. Energy & Environ Sci 2014;7:3801–7.
[21] Yao Q, Chen LD, Zhang WQ, Liufu SC, Chen XH. Enhanced thermoelectric performance of single-walled carbon nanotubes/polyaniline hybrid nanocomposites. Acs Nano 2010;4:2445–51.
[22] Meng CZ, Liu CH, Fan SS. A promising approach to enhanced thermoelectric properties using carbon nanotube networks. Adv Mater 2010;22:535–9.
[23] See KC, Feser JP, Chen CE, Majumdar A, Urban JJ, Segalman RA. Water-processable polymer-nanocrystal hybrids for thermoelectrics. Nano Lett 2010;10:4664–7.
[24] Zhang K, Zhang Y, Wang SR. Effectively decoupling electrical and thermal conductivity of polymer composites. Carbon 2013;65:105–11.
[25] Zhang K, Davis M, Qiu JJ, Hope-Weeks L, Wang SR. Thermoelectric properties of porous multi-walled carbon nanotube/polyaniline core/shell nanocomposites. Nanotechnology 2012;23. 385701.
[26] Wang Y, Zhang SM, Deng Y. Flexible low-grade energy utilization devices based on high-performance thermoelectric polyaniline/tellurium nanorod hybrid films. J Mater Chem 2016;A 4:3554–9.
[27] Yee SK, Coates NE, Majumdar A, Urban JJ, Segalman RA. Thermoelectric power factor optimization in PEDOT: PSS tellurium nanowire hybrid composites. Phys Chem Chem Phys 2013;15:4024–32.

[28] Yang Y, Lin ZH, Hou T, Zhang F, Wang ZL. Nanowire-composite based flexible thermoelectric nanogenerators and self-powered temperature sensors. Nano Res 2012;5:888–95.
[29] Ju H, Kim J. Fabrication of conductive polymer/inorganic nanoparticles composite films: PEDOT: PSS with exfoliated tin selenide nanosheets for polymer-based thermoelectric devices. Chem Eng J 2016;297:66–73.
[30] Ju H, Kim J. Chemically exfoliated snse nanosheets and their snse/poly(3,4-ethylenedioxythiophene):poly(styrenesulfonate) composite films for polymer based thermoelectric applications. Acs Nano 2016;10:5730–9.
[31] Chatterjee K, Mitra M, Kargupta K, Ganguly S, Banerjee D. Synthesis, characterization and enhanced thermoelectric performance of structurally ordered cable-like novel polyaniline-bismuth telluride nanocomposite. Nanotechnology 2013;24. 215703.
[32] He M, Ge J, Lin Z, Feng X, Wang X, Lu H, et al. Thermopower enhancement in conducting polymer nanocomposites via carrier energy scattering at the organic-inorganic semiconductor interface. Energy & Environ Sci 2012;5:8351–8.
[33] Zhang B, Sun J, Katz HE, Fang F, Opila RL. Promising thermoelectric properties of commercial pedot: pss materials and their bi2te3 powder composites. Acs Appl Mater Interfaces 2010;2:3170–8.
[34] Wang LM, Yao Q, Xiao JX, Zeng KY, Qu SY, Shi W, et al. Engineered molecular chain ordering in single-walled carbon nanotubes/polyaniline composite films for high-performance organic thermoelectric materials. Chemistry-An Asian J 2016;11:1804–10.
[35] Wang H, Yi S-i, Pu X, Yu C. Simultaneously improving electrical conductivity and thermopower of polyaniline composites by utilizing carbon nanotubes as high mobility conduits. Acs Appl Mater Interfaces 2015;7:9589–97.
[36] Bounioux C, Diaz-Chao P, Campoy-Quiles M, Martin-Gonzalez MS, Goni AR, Yerushalmi-Rozen R, et al. Thermoelectric composites of poly(3-hexylthiophene) and carbon nanotubes with a large power factor. Energy & Environ Sci 2013;6:918–25.
[37] Yu C, Choi K, Yin L, Grunlan JC. Light-Weight flexible carbon nanotube based organic composites with large thermoelectric power factors. Acs Nano 2011;5:7885–92.
[38] Xiong JH, Jiang FX, Shi H, Xu JK, Liu CC, Zhou WQ, et al. Liquid exfoliated graphene as dopant for improving the thermoelectric power factor of conductive pedot: pss nanofilm with hydrazine treatment. Acs Appl Mater Interfaces 2015;7:14917–25.
[39] Wang L, Yao Q, Bi H, Huang F, Wang Q, Chen L. PANI/graphene nanocomposite films with high thermoelectric properties by enhanced molecular ordering. J Mater Chem 2015;A 3:7086–92.
[40] Yoo D, Kim J, Kim JH. Direct synthesis of highly conductive poly(3,4-ethylenedioxythiophene):poly(4-styrenesulfonate) (PEDOT: PSS)/graphene composites and their applications in energy harvesting systems. Nano Res 2014;7:717–30.
[41] Wang L, Yao Q, Shi W, Qu S, Chen L. Engineering carrier scattering at the interfaces in polyaniline based nanocomposites for high thermoelectric performances. Mater Chem Front 2017;1:741–8.
[42] Zhang K, Qiu JJ, Wang SR. Thermoelectric properties of PEDOT nanowire/PEDOT hybrids. Nanoscale 2016;8:8033–41.
[43] Choi J, Lee JY, Lee S-S, Park CR, Kim H. High-performance thermoelectric paper based on double carrier-filtering processes at nanowire heterojunctions. Adv Energy Mater 2016;6. 1502181.
[44] Cho C, Wallace KL, Tzeng P, Hsu J-H, Yu C, Grunlan JC. Outstanding low temperature thermoelectric power factor from completely organic thin films enabled by multidimensional conjugated nanomaterials. Adv Energy Mater 2016;6. 1502168.
[45] Bae EJ, Kang YH, Jang KS, Cho SY. Enhancement of Thermoelectric properties of pedot: pss and tellurium-pedot: pss hybrid composites by simple chemical treatment. Sci Rep 2016;6. 18805.
[46] Suemori K, Watanabe Y, Hoshino S. Carbon nanotube bundles/polystyrene composites as high-performance flexible thermoelectric materials. Appl Phys Lett 2015;106.
[47] Hong CT, Lee W, Kang YH, Yoo Y, Ryu J, Cho SY, et al. Effective doping by spin-coating and enhanced thermoelectric power factors in SWCNT/P3HT hybrid films. ournal Mater Chem 2015;A 3:12314–9.
[48] Cho C, Stevens B, Hsu J-H, Bureau R, Hagen DA, Regev O, et al. Completely organic multilayer thin film with thermoelectric power factor rivaling inorganic tellurides. Adv Mater 2015;27:2996–3001.
[49] Coates NE, Yee SK, McCulloch B, See KC, Majumdar A, Segalman RA, et al. Effect of interfacial properties on polymer-nanocrystal thermoelectric transport. Adv Mater 2013;25:1629–33.
[50] Ma S, Anderson K, Guo L, Yousuf A, Ellingsworth EC, Vajner C, et al. Temperature dependent thermopower and electrical conductivity of Te nanowire/poly(3,4-ethylenedioxythiophene):poly(4-styrene sulfonate) microribbons. Appl Phys Lett 2014;105. 073905.
[51] Jiang F, Xiong J, Zhou W, Liu C, Wang L, Zhao F, et al. Use of organic solvent-assisted exfoliated MoS2 for optimizing the thermoelectric performance of flexible PEDOT: PSS thin films. J Mater Chem 2016;A 4:5265–73.
[52] Zaia EW, Sahu A, Zhou P, Gordon MP, Forster JD, Aloni S, et al. Carrier scattering at alloy nanointerfaces enhances power factor in PEDOT: PSS hybrid thermoelectrics. Nano Lett 2016;16:3352–9.
[53] Lee D, Sayed SY, Lee S, Kuryak CA, Zhou J, Chen G, et al. Quantitative analyses of enhanced thermoelectric properties of modulation-doped PEDOT: PSS/undoped Si (001) nanoscale heterostructures. Nanoscale 2016;8:19754–60.
[54] Wang L, Yao Q, Bi H, Huang F, Wang Q, Chen L. Large thermoelectric power factor in polyaniline/graphene nanocomposite films prepared by solution-assistant dispersing method. J Mater Chem 2014;A 2:11107–13.
[55] Lee W, Kang YH, Lee JY, Jang KS, Cho SY. Improving the thermoelectric power factor of CNT/PEDOT: PSS nanocomposite films by ethylene glycol treatment. Rsc Adv 2016;6:53339–44.
[56] Li F, Cai K, Shen S, Chen S. Preparation and thermoelectric properties of reduced graphene oxide/PEDOT: PSS composite films. Synth Met 2014;197:58–61.
[57] Zhang K, Wang SR, Zhang X, Zhang Y, Cui Y, Qiu JJ. Thermoelectric performance of p-type nanohybrids filled polymer composites. Nano Energy 2015;13:327–35.
[58] Lu GH, Bu LJ, Li SJ, Yang XN. Bulk interpenetration network of thermoelectric polymer in insulating supporting matrix. Adv Mater 2014;26:2359–64.
[59] Shi H, Liu CC, Xu JK, Song HJ, Lu BY, Jiang FX, et al. Facile fabrication of PEDOT: PSS/Polythiophenes bilayered nanofilms on pure organic electrodes and their thermoelectric performance. Acs Appl Mater Interfaces 2013;5:12811–9.
[60] Lee HJ, Anoop G, Kim C, Park JW, Choi J, Kim H, et al. Enhanced thermoelectric performance of PEDOT: PSS/PANI-CSA polymer multilayer structures. Energy & Environ Sci 2016;9:2806–11.
[61] Yu C, Kim YS, Kim D, Grunlan JC. Thermoelectric behavior of segregated-network polymer nanocomposites. Nano Lett 2008;8:4428–32.
[62] Yu B, Zebarjadi M, Wang H, Lukas K, Wang HZ, Wang DZ, et al. Enhancement of thermoelectric properties by modulation-doping in silicon germanium alloy nanocomposites. Nano Lett 2012;12:2077–82.
[63] Zebarjadi M, Joshi G, Zhu GH, Yu B, Minnich A, Lan YC, et al. Power factor enhancement by modulation doping in bulk nanocomposites. Nano Lett 2011;11:2225–30.
[64] Xu H, Pang XC, He YJ, He M, Jung JH, Xia HP, et al. An Unconventional route to monodisperse and intimately contacted semiconducting organic-inorganic nanocomposites. Angew Chemie-International Ed 2015;54:4636–40.
[65] Abad B, Alda I, Diaz-Chao P, Kawakami H, Almarza A, Amantia D, et al. Improved power factor of polyaniline nanocomposites with exfoliated graphene nanoplatelets (GNPs). J Mater Chem 2013;A 1:10450–7.
[66] Kim D, Kim Y, Choi K, Grunlan JC, Yu CH. Improved thermoelectric behavior of nanotube-filled polymer composites with Poly(3,4-ethylenedioxythiophene) Poly(styrenesulfonate). Acs Nano 2010;4:513–23.
[67] Wang Q, Yao Q, Chang J, Chen LD. Enhanced thermoelectric properties of CNT/PANI composite nanofibers by highly orienting the arrangement of polymer chains. J Mater Chem 2012;22:17612–8.
[68] Liu JL, Sun J, Gao L. Flexible single-walled carbon nanotubes/polyaniline composite films and their enhanced thermoelectric properties. Nanoscale 2011;3:3616–9.
[69] Xu K, Chen G, Qiu D. Convenient construction of poly(3,4-ethylenedioxythiophene)-graphene pie-like structure with enhanced thermoelectric performance. J Mater Chem 2013;A 1:12395–9.
[70] Lu Y, Song Y, Wang FP. Thermoelectric properties of graphene nanosheets-modified polyaniline hybrid nanocomposites by an in situ chemical polymerization. Mater Chem Phys 2013;138:238–44.
[71] Kim GH, Hwang DH, Woo SI. Thermoelectric properties of nanocomposite thin films prepared with poly(3,4-ethylenedioxythiophene) poly(-styrenesulfonate) and graphene. Phys Chem Chem Phys 2012;14:3530–6.
[72] Wei QS, Mukaida M, Kirihara K, Naitoh Y, Ishida T. Recent progress on PEDOT-based thermoelectric materials. Materials 2015;8:732–50.
[73] Mai CK, Liu J, Evans CM, Segalman RA, Chabinyc ML, Gahill DG, et al. Anisotropic thermal transport in thermoelectric composites of conjugated polyelectrolytes/single-walled carbon nanotubes. Macromolecules 2016;49:4957–63.
[74] Chen J, Wang L, Gui X, Lin Z, Ke X, Hao F, et al. Strong anisotropy in thermoelectric properties of CNT/PANI composites. Carbon 2017;114:1–7.
[75] Madan D, Wang ZQ, Chen A, Juang RC, Keist J, Wright PK, et al. Enhanced performance of dispenser printed MA n-type Bi2Te3 composite thermoelectric generators. Acs Appl Mater Interfaces 2012;4:6117–24.
[76] Wei K, Stedman T, Ge ZH, Woods LM, Nolas GS. A synthetic approach for enhanced thermoelectric properties of PEDOT: PSS bulk composites. Appl Phys Lett 2015;107. 153301.
[77] Madan D, Wang ZQ, Chen A, Wright PK, Evans JW. High-Performance dispenser Printed MA p-Type Bi0.5Sb1.5Te3 flexible thermoelectric generators for powering wireless sensor networks. Acs Appl Mater Interfaces 2013;5:11872–6.
[78] Wang YY, Cai KF, Yao X. One-pot fabrication and enhanced thermoelectric properties of poly(3,4-ethylenedioxythiophene)-Bi2S3 nanocomposites. J Nanoparticle Res 2012;14:848.
[79] Wang YY, Cai KF, Yin JL, An BJ, Du Y, Yao X. In situ fabrication and thermoelectric properties of PbTe-polyaniline composite nanostructures. J Nanoparticle Res 2011;13:533–9.
[80] Taylor PS, Korugic-Karasz L, Wilusz E, Lahti PM, Karasz FE. Thermoelectric studies of oligophenylenevinylene segmented block copolymers and their blends with MEH-PPV. Synth Met 2013;185:109–14.
[81] Zhang K, Wang S, Qiu J, Blackburn JL, Zhang X, Ferguson AJ, et al. Effect of host-mobility dependent carrier scattering on thermoelectric power factors of polymer composites. Nano Energy 2016;19:128–37.
[82] Menon AK, Meek O, Eng AJ, Yee SK. Radial thermoelectric generator fabricated from n- and p-type conducting polymers. J Appl Polym Sci 2017;134. 44060.
[83] Fang H, Popere BC, Thomas EM, Mai C-K, Chang WB, Bazan GC, et al. Large-

scale integration of flexible materials into rolled and corrugated thermoelectric modules. J Appl Polym Sci 2017;134. 44208.
[84] Zhang Z, Qiu J, Wang S. Roll-to-roll printing of flexible thin-film organic thermoelectric devices. Manuf Lett 2016;8:6–10.
[85] Li P, Guo Y, Mu JK, Wang HZ, Zhang QH, Li YG. Single-walled carbon nanotubes/polyaniline-coated polyester thermoelectric textile with good interface stability prepared by ultrasonic induction. Rsc Adv 2016;6: 90347–53.
[86] Bae EJ, Kang YH, Jang KS, Lee C, Cho SY. Solution synthesis of telluride-based nano-barbell structures coated with PEDOT: PSS for spray-printed thermoelectric generators. Nanoscale 2016;8:10885–90.
[87] Hong CT, Kang YH, Ryu J, Cho SY, Jang KS. Spray-printed CNT/P3HT organic thermoelectric films and power generators. J Mater Chem 2015;A 3: 21428–33.
[88] Du Y, Cai K, Chen S, Wang H, Shen SZ, Donelson R, et al. Thermoelectric fabrics: toward power generating clothing. Sci Rep 2015;5:6411.
[89] Suemori K, Hoshino S, Kamata T. Flexible and lightweight thermoelectric generators composed of carbon nanotube-polystyrene composites printed on film substrate. Appl Phys Lett 2013;103. 153902.
[90] Hewitt CA, Montgomery DS, Barbalace RL, Carlson RD, Carroll DL. Improved thermoelectric power output from multilayered polyethylenimine doped carbon nanotube based organic composites. J Appl Phys 2014;115. 184502.
[91] Hewitt CA, Kaiser AB, Roth S, Craps M, Czerw R, Carroll DL. Multilayered carbon nanotube/polymer composite based thermoelectric fabrics. Nano Lett 2012;12:1307–10.
[92] Orrill M, LeBlanc S. Printed thermoelectric materials and devices: fabrication techniques, advantages, and challenges. J Appl Polym Sci 2017;134. 44256.
[93] Jiao F, Di CA, Sun YM, Sheng P, Xu W, Zhu DB. Inkjet-printed flexible organic thin-film thermoelectric devices based on p- and n-type poly(metal 1,1,2,2-ethenetetrathiolate)s/polymer composites through ball-milling. Philosophical Trans R Soc a-Mathematical Phys Eng Sci 2014;372. 20130008.